The Mechanics of Plant Morphogenesis

Enrico Coen[1] and Daniel J. Cosgrove[2]

[1]Department of Cell and Developmental Biology, John Innes Centre, Norwich Research Park, Colney Lane, Norwich, NR4 7UH, UK

[2] Department of Biology, Pennsylvania State University, University Park, PA 16870 USA

Teaser

Interactions between fibers in plant cell walls can lead to the generation of complex tissue shapes.

Abstract

Understanding the mechanism by which patterned gene activity leads to mechanical deformation of cells and tissues to create complex forms is a major challenge for developmental biology. Plants offer advantages for addressing this problem because their cells do not migrate or rearrange during morphogenesis, simplifying analysis. We synthesize results from experimental analysis and computational modelling to show how mechanical interactions between cellulose fibers translate through wall, cell and tissue levels to generate complex plant tissue shapes. Genes can modify mechanical properties and stresses at each level, though the values and pattern of stresses differ from one level to the next. The dynamic cellulose network provides elastic resistance to deformation while allowing growth through fiber sliding, enabling morphogenesis while maintaining mechanical strength.

Introduction

The growth and shape of plants depend on the mechanical properties of the plant's mesh of interconnected cell walls. Because adhering cell walls prevent cell migrations, morphogenesis is simpler to study in plants than in animals. Spatiotemporal variations in the rates and orientations at which cell walls yield to mechanical stresses – ultimately powered by cell turgor pressure – underlie the development and diversity of plant forms. Considerable progress has been made in understanding the molecular genetic basis of plant morphogenesis, but confusion and controversies remain over how these findings relate to the mechanics of development. Here we review new insights and points of current contention in our understanding of the mechanics of plant morphogenesis, starting from wall components and building up to cells and tissues.

At the heart of morphogenesis is a trade-off between mechanical stiffness and deformability. As a plant develops it must resist external mechanical forces, such as gravity and wind, while also growing by several orders of magnitude and deforming to produce its characteristic shapes. Plant materials therefore need to be strong while also pliant enough to grow and deform. These conflicting requirements are partly met by restricting morphogenesis to protected areas such as embryos, growing tips (apical meristems), and cambial zones, reducing the extent to which they weaken the plant. However, even within these zones, mechanical strength needs to be maintained. A key problem is how such strength is achieved in the face of growth.

Fiber Mechanics

The mechanical properties of plant tissues largely depend on how fibers in cell walls are organised. These fibers experience tensile stress caused by turgor pressure of several atmospheres within each cell, which provides the primary driving force for plant growth (*1-3*). Non-turgor-based mechanisms,

in which growth is driven by active insertion of cell wall material, have been proposed (*4, 5*), but their contribution to plant growth remains contentious (*1, 6*).

The main load-bearing fibers are cellulose microfibrils, each comprising many linear β1,4-glucan chains packed into a crystalline array, with stiffness comparable to steel. Aligned microfibrils bind strongly to each other laterally, forming 2D networks that resist being stretched (*7*). Microfibrils are embedded in a hydrophilic matrix of pectins and hemicelluloses that comprise most of the cross-sectional area of the growing cell wall, yet bear little tensile stress (*8*).

We first consider growth in one dimension. Wall growth involves two types of fiber stress: tensile and shear. If a tensile force F is applied to a fiber of length L and causes extension by ΔL, the proportionate increase in length, or fiber strain, is defined as $\varepsilon_f = \Delta L/L$. For an idealized linear elastic fiber, fiber strain is proportional to fiber tensile stress, $\sigma_f = F/A_f$, where A_f is the fiber cross-sectional area (Fig. 1A, B). The constant of proportionality is $1/E_f$, where E_f is Young's modulus of the fiber. If we introduce a second fiber in parallel and apply the same force, the tensile stress in each fiber is halved and fiber strain is halved (Fig. 1C), as is the strain of the entire structure or wall ε_w. Thus, for a given tensile force, stress and strain are inversely proportional to fiber number, N. Because of the proportionality between wall strain and fiber tensile stress, strain in cellular components that deform together with the wall, such as the plasma membrane or cortex, can be used to infer fiber stress (Movie 1).

If fibers are firmly stuck together at an interface along their length and force is applied to only one end of each fiber (Fig. 1D), a shear stress, τ_f, acts at the interface. Shear stress equals F/A_c, where A_c is the contact area along the length of the fibers. As fiber number N increases, there are more fibers and interfaces to resist the tensile force, so τ_f and σ_f decrease. As above, plasma membrane or cortical strain can be used to infer σ_f (Movie 2).

So far, we have assumed an elastic regime in which all deformations are reversible. Cell wall enlargement during growth, however, is largely irreversible, arising through slow sliding of the fiber network. Suppose τ_f exceeds a slippage threshold, such that sliding occurs at the fiber interface (yellow, Fig. 1E). In this situation, wall strain, ε_w, is no longer proportional to stress because wall strain continually increases in time while stress does not. Thus, plasma membrane or cortical strain can no longer be used to infer fiber tensile stress (Movie 3). For a simple linear case, the rate of increase in ε_w, or strain rate, $\dot{\varepsilon}_w$, is proportional to shear stress above the slippage threshold. The constant of proportionality, a type of "extensibility", depends on the strength with which fibers adhere to each other (i.e. fiber-fiber binding energy). If forces are removed, individual fibers relax to their resting lengths but wall strain due to slippage does not reverse.

From Fibers to Walls

A simplified mechanical view of a growing cell wall is a network of overlapping cellulose microfibrils sticking to each other and stretched by a turgor-based tensional force F, maintained by cellular water uptake (Fig. 2A). Irreversible wall enlargement (~5-10%/h in rapidly growing tissue) occurs at ~constant turgor pressure through slow microfibril sliding, facilitated by a nonenzymatic wall-loosening protein, expansin (*9*). As the growing wall thins through extension, wall thickness is maintained by addition of new microfibrils (red, Fig. 2B), synthesised at the plasma membrane, together with incorporation of additional matrix materials. Each nascent microfibril begins to bear tensile load when it binds to overlying microfibrils it straddles, becoming part of the cohesive cellulose network. As the overlying microfibrils slide, the nascent fiber is put under tension, "taking up the slack".

This simplified account is consistent with the structure and nanoscale mechanics of primary cell walls (*10, 11*), but omits the mechanical role of matrix polysaccharides. Hemicelluloses, such as xyloglucan, bind strongly to cellulose surfaces in extended conformations and as random coils, whereas pectins form a soft hydrogel that binds weakly to cellulose surfaces (*12-14*). Micro-indentation measurements of various growing organs and pectin-rich pollen tubes have implicated pectins in the control of wall stiffness (*15*), while other experimental and computational results indicate that tensile stress is borne mainly by the cellulose network, with minor contribution by matrix polymers (*8, 16*). The apparent contradiction may be partly resolved by recognition that in-plane stretching of walls involves different modes of polymer deformation than out-of-plane indentation (*12*), with the cellulose network dominating in-plane tensile stretching while pectins contribute substantially to out-of-plane mechanics (*16, 17*). Pectins and xyloglucan may also influence tensile mechanics indirectly by modulating the formation of cellulose-cellulose contacts during wall assembly and remodelling, thereby shaping the cellulose network and its mechanical properties (*12*). Another proposal is that enzymatic swelling of pectin may supply an additional driving force for wall enlargement (*14*).

In addition to their structural role, pectins and xyloglucan participate in local signalling by auxin and brassinosteroid (*18-20*), influencing many downstream pathways. Direct mechanical effects of these matrix polysaccharides may therefore be confounded with indirect hormonal responses, complicating the interpretation of genetic studies, and possibly accounting for divergent views on the effects of pectin modifications (*12-14, 21-24*). The role of pectins in wall mechanics and growth therefore remains contentious and further results will be needed to reach a unified view.

In growing cell walls, lateral interfaces between aligned cellulose microfibrils are heterogeneous, involving direct cellulose-cellulose contacts, contacts mediated by a thin layer of water, and bonding through a monolayer of hemicelluloses (*12, 25*). The relative importance of these different interfaces for cellulose slippage has not been established. The major endogenous catalysts of cell wall extension, α-expansins, loosen noncrystalline cellulose-cellulose interactions *in vitro* (*9*), but molecular details are lacking. The loosening action of α-expansins may be restricted to infrequent sites of slippage, dubbed 'biomechanical hotspots" (*12, 26*). Tethering between cellulose microfibrils by xyloglucan may also occur, but contributes little to steady-state tensile mechanics (*8, 26*). However, mechanical responses of isolated cell walls to exogenous β1,4-endoglucanases implicate regions of intertwined cellulose-xyloglucan in limiting cellulose sliding (*16, 26*).

We may also consider the wall as a continuous material. From this perspective, wall stress, σ_w, equals F/A_w, where A_w is the wall cross-sectional area. Wall stress is less than fiber stress, as matrix contributes to the cross-sectional wall area, while not bearing the main tensile load (*8*). Microfibril sliding, facilitated by α-expansin, can account for wall creep, readily observed as slow, irreversible extension of a wall held at constant force above a yield threshold (the minimum where creep begins) (*9*). Such sliding can dissipate wall stresses, termed wall stress relaxation, which is most apparent when wall enlargement is physically constrained (*12*). Stress relaxation generates the slight water potential disequilibrium required for sustained water uptake during cell enlargement (*27*). The stimulation of wall stress relaxation and creep by α-expansins is maximal at acidic pH and entails changes in both the strain-rate proportionality constant, commonly called "wall extensibility" (*2*), and the yield threshold (*28*). This pH dependence enables rapid and local control of wall loosening by a signaling pathway that activates plasma membrane H^+-ATPases, which acidify the wall space to activate α-expansins and promote wall creep (*29*). The biological control of wall pH and thereby expansin activity – which does not occur in mechanical measurements of isolated cell walls – may

result in dynamic shifts in wall extensibility and yield threshold observed *in vivo* (*3, 30*), consistent with pH-dependent expansin action measured *in vitro* (*28*).

In addition to elasticity and creep, cell walls may also display plasticity, observable as an immediate irreversible deformation when tensile force is suddenly increased beyond a threshold (*9, 31*). While both plasticity and creep involve cellulose-cellulose sliding, they differ in timescale and microsites of cellulose movements. Plastic deformation, unlike wall creep, is nearly independent of time and expansins and does not occur during normal cell growth, which occurs at steady turgor (steady wall stress). Sudden changes in wall tensile force (e.g. in a mechanical tester) also reveal transient mechanical responses termed viscoelastic or viscoplastic deformations. These are material responses that generally subside within a few minutes of the change in force, reflecting the short time constants of most physical rearrangements of matrix polymers and the cellulose network (other than expansin-mediated creep). Developmental patterns of wall or tissue viscoelasticity/plasticity are sometimes associated with growth (*1, 15, 23*), but in other cases the correlations are poor or nonexistent (*12, 32*). Consequently, the interpretation of viscoelastic-plastic measurements in relation to wall growth is a point of contention. Contrasting ideas of cell wall structure and whether tensile forces are transmitted between cellulose fibers via direct cellulose-cellulose contacts or via matrix polysaccharides lie at the heart of these divergent views (*12*).

Wall synthesis and loosening influence cell growth via wall creep in complementary ways (*33, 34*). Wall loosening increases growth rate with almost immediate effect (*35*), but unless wall synthesis increases in parallel, wall thickness declines over time, potentially weakening the wall. Wall synthesis requires a longer timescale to have a discernible growth effect but is critical for maintaining wall thickness and orienting anisotropy (see below). By regulating loosening and synthesis separately, plants have the flexibility to produce rapid growth responses as well as control longer term growth patterns and mechanical strength.

Anisotropic Wall Growth

Plant morphogenesis involves differential orientations and rates of growth. Such growth anisotropy is evident at the wall level, as shown by marking walls of the classically-studied alga *Nitella axillaris*, whose internodes are one cell wide and grow about four times faster in length than circumference (*36, 37*). A key question is how growth anisotropy is determined and regulated.

Growth anisotropy depends on the three-dimensional structure of the cell wall. Consider a square piece of wall with two layers of microfibrils (color-coded blue and red in Fig. 3A), oriented perpendicular to each other. A tensile force, F, is applied to the ends of the wall equally in both microfibril orientations. If microfibrils are the main load-bearing components, the average microfibril stress σ_f equals F/NA_f, where N is the number of microfibrils in the cross-section. Without microfibril slippage, wall strain, ε_w, equals fiber strain, ε_f, and is the same in both orientations. As F increases, shear stress may exceed the slippage threshold and the wall grows at a strain rate, $\dot{\varepsilon}_w$, which is the same in both orientations, giving isotropic growth.

To introduce anisotropy, we add a second layer of blue microfibrils (Fig. 3B). There are now half as many red microfibrils resisting the red force as blue resisting the blue force, so red tensile stress is twice that of blue. Red microfibrils are also under twice the shear stress of blue. As F increases, microfibrils begin to slip and exhibit faster slippage in the red compared to the blue direction. Thus, the orientation of maximal growth rate is aligned with the orientation of maximal microfibril stress.

Yet from a continuum perspective, wall stress, σ_w, is equal in both orientations, as A_w is the same for each (Fig. 3C). The wall Young's modulus and yield threshold (proportional to fiber slippage

threshold x *N*) are twice in the blue direction compared to red. As *F* increases, the wall begins to yield and exhibits faster creep in the red direction compared to blue. Thus, from a continuum perspective, direction of maximal growth is coaligned with the direction of lowest Young's modulus and wall yield threshold, whereas from a fiber perspective, maximal growth occurs in the direction of highest microfibril stress.

From Walls to Cells

Modulation of wall properties can lead to formation of diverse cell geometries (*38*). Cell geometry may in turn feed back to influence stresses (*39*). In a turgid spherical cell with isotropic walls, tensile stresses are equal in all directions in the plane of the wall. However, in a cylindrical cell with isotropic walls, both wall stress and microfibril stress are twice in the circumferential compared to axial direction (*40*), which would lead to greater growth in cell diameter than length. Yet elongated cells often exhibit axial growth. Such growth may be achieved through preferential loosening and synthesis of the wall at one end: tip growth (*41*). However, the cylindrical internode cells of *Nitella* grow faster axially than circumferentially even though growth is distributed throughout the wall: diffuse growth (*36*). Diffuse growth is common to most cells of the plant body (*42*).

Diffuse axial growth can be explained by wall anisotropy. Assume the wall of the cylindrical cell has twice as many circumferential microfibrils as axial (Fig. 4). Although tensile force is twice in the circumferential orientation (blue arrows), there are twice as many microfibrils to resist it, and therefore microfibril stress is equal in both orientations. The wall will therefore grow equally along both the circumferential and axial directions. If the number of circumferential microfibrils is more than twice axial, microfibril stress will be higher in the axial orientation and the cell grows faster in length than circumference. From a continuum perspective, resistance to wall creep is more than twice in the circumferential compared to axial direction, leading to low circumferential growth despite twice the wall stress. Measurements on *Nitella* internode cells confirm that they have a greater proportion of circumferential to axial microfibrils, and have more than twice the wall yield stress threshold in the circumferential orientation (*36, 37, 43, 44*).

Control of Microtubule Orientation in Individual Cells

Microfibril orientation is primarily determined by microtubules guiding cellulose synthases (*45*), although feedback from microfibrils can also guide cellulose synthases where microtubules are absent (*46*). When the growing end of a microtubule collides with another microtubule, it may turn to follow the microtubule (zippering) or undergo depolymerisation (collision-induced catastrophe) (*47*). Computer simulations show that such interactions in a population of microtubules can generate alignments (i.e. near-parallel arrangements) that maximise microtubule survival probability (*48, 49*). In a spherical cell without cues, such alignments are randomly oriented. For an elongated cell, orientations along the cell's long axis can be favoured by microtubule severing, consistent with longitudinal microtubule orientations observed in wall-less plant cells (protoplasts) deformed in rectangular microwells (*50*).

The predominant microtubule orientation in microwell-constrained protoplasts changes from longitudinal to transverse under high turgor, which has been explained by microtubules responding to the direction of maximal tension in the cell cortex (*51*). There has been confusion, however, over how stress-sensing in the cell cortex relates to sensing stresses in the wall. Stress-sensing depends on cells being able to sense strain (*31*), which is proportional to stress for elastic deformations (Fig. 1 A-D). Thus, for elastic deformations, cortical stress/strain can be a proxy for measuring wall stress (Movies 1 and 2). However, in a walled cell which grows by creep, strain and wall stress are not proportional (strain can increase for a fixed stress, Fig. 1E, Movie 3). The direction of maximal strain

221 therefore need not correspond to the direction of maximal wall stress (e.g. axially-growing
222 cylindrical cell). Thus, for an intact growing plant cell, stress-sensing in the cortex relates to wall
223 strain, not wall stress. In principle, sudden changes in wall stress could be detected by
224 membrane/cortical strain, because creep is slow, but the relevance of such rapid stress changes to
225 plant growth, which occurs under steady turgor, is unclear.

226 Various hypotheses have been proposed for how microtubules, and thus microfibrils, are oriented in
227 intact plant cells. Classic studies on cylindrical *Nitella* cells suggested microtubules are aligned
228 passively by early-stage circumferential growth (*52*). This model was later disproved, leading to the
229 hypothesis that microfibrils determine the directionality of cell expansion in accord with wall stress
230 (*37*). One hypothesis is that membrane-spanning receptors have two domains: an extracellular
231 domain that preferentially binds to more highly stressed microfibrils, and an intracellular domain
232 that binds to microtubules, aligning them with the direction of the bound microfibrils (*53*). By
233 connecting to both microfibrils and microtubules, such receptors would allow the direction of the
234 maximal wall stress to orient microtubules, avoiding the problem of indirect sensing via cortical or
235 plasma membrane strain. However, enzymatic treatments or mutants that modify mechanical
236 properties of walls by interfering with cellulose content have no discernible effect on microtubule
237 patterning (*54, 55*), which argues against this mechanism.

238 Another microtubule-orienting hypothesis is based on asymmetric localisation of molecules across a
239 cell, as exhibited by several plant polarity proteins (*56-62*). A cell polarity protein in protoplasts was
240 found to align with their subsequent growth orientation (*63*). Computer simulations show that
241 microtubules tend to adopt orientations parallel to faces or edges where they are preferentially
242 destabilised, as such orientations increase microtubule survival probability (*48, 64*). If polarity
243 proteins at opposite end-faces or edges of a cylindrical cell destabilise microtubules, microtubule
244 orientations parallel to the edges (i.e. circumferential) would therefore be favoured. This hypothesis
245 remains to be further explored.

246 Microtubule-orienting mechanisms have also been investigated for jigsaw puzzle-shaped epidermal
247 cells (pavement cells). Microtubules on the outer face of these cells form arrays that fan out from
248 the neck tips, which has been explained through response to stresses, localized protein activity
249 and/or cell geometry (*65*).

250 From Cells to Tissues

251 Morphogenesis of multicellular tissues depends not only on properties of individual cells but also on
252 mechanical interactions between them. Consider a spherical turgid cell with isotropic walls that
253 undergoes division (Fig. 5A, B). With strong adhesion at the middle lamella (m, yellow), the cells
254 would grow to form two partial spheres joined by a flat interface (Fig. 5C). With reduced adhesion, a
255 degree of cell separation may occur, leading to two spherical daughters in the extreme case. The
256 extent of cell-cell adhesion is influenced by wall matrix components, such as pectins (*66*).

257 Suppose our cells continue to grow, divide and adhere to form a spherical tissue (Fig. 5D), with an
258 epidermal layer (grey) and all cells maintaining the same turgor. All walls have the same thickness,
259 isotropic material properties and similar tensile stress. However, if the outer epidermal walls are
260 thicker (purple, Fig. 5F), as is common for many tissues, tensile stress is reduced in these walls
261 because their cross-sectional area, A_w, is greater. The outer walls therefore create a growth
262 constraint. Turgor force is then transferred from inner to outer walls, increasing the tensile force on
263 outer walls.

264 Such tensile forces, or tissue tensions, have been inferred from the way tissues bend or gape after
265 being cut, or by the formation of epidermal cracks when adhesion between cells is weakened (*67-*
266 *69*). Tissue tension can be quantified by stretching detached epidermal tissue to the point that it
267 restores its original length (*70*). Epidermal tissue tension is counterbalanced by internal tissue
268 compression – internal tissue expands when the epidermal constraint is removed. Thus, tissue
269 stresses can be either tensile or compressive. They impose additional forces on cells that can
270 increase or decrease wall stresses, as a result of connectivity with other cells with different
271 mechanical/growth properties (*71*).

272 Just as wall stress is based on the notion of a continuous wall, tissue stress is based on the notion of
273 a continuous tissue (*70, 72*). If all regions of a continuous uniformly growing sphere have the same
274 isotropic mechanical and growth properties, there are no tissue stresses (corresponding to all cell
275 walls having the same thickness and wall stress). However, if the outer region of the sphere (purple
276 in Fig. 5F) is more resistant to growth (e.g. because of thick outer cell walls), the tissue effectively
277 behaves as a continuous pressurized vessel, with the outer region under tissue tension and the inner
278 region under tissue compression (*73*) (Fig. 5F). Tissue stress does not equate to wall stress: although
279 tensile tissue stress is higher in the outer region, outer wall tensile stress may be reduced because of
280 elevated A_w. Similarly, although the inner region is under tissue compression, inner cell walls may
281 partially resist some turgor force and thus be stretched in tension.

282 If the tissue has the form of a cylinder, thickened outer walls will lead to circumferential tissue
283 tension being twice axial. Outer wall and fiber stresses will also be greater in the circumferential
284 orientation, resulting in axial cracks when cell adhesion is compromised, as observed with shoot
285 apices (*68*).

286 So far, we have assumed cell walls in our tissue have isotropic properties. Each cell would therefore
287 grow spherically if mechanically isolated from its neighbours. If walls have anisotropic properties
288 (e.g. biased microfibril orientations), cells in mechanical isolation would grow to form other shapes,
289 such as ellipsoids. Oriented tissue growth may arise by coordination of such growth anisotropies
290 between cells. For instance, if cell growth of interior cells is preferentially axial for a cylindrical
291 tissue, thicker outer cell walls would lead to axial outer tissue tension and axial inner tissue
292 compression (*72*) (Fig. 5G), as observed in hypocotyls (*67-69*). Growth anisotropy of hypocotyls may
293 be enhanced through increasing wall extensibility by brassinosteroid (*32*) or by selective weakening
294 of axial walls (*23*).

295 Correlation between Tissue Stresses and Microtubule Orientations

296 In multicellular tissues, microtubules are typically aligned with maximal tissue tension (*74, 75*). For
297 example, in shoot apical meristems, microtubules are oriented circumferentially around the apex
298 and are aligned with organ-meristem junctions, the predicted orientation of maximal tissue tension
299 (*73*). Wounding leads to microtubules orienting circumferentially around the wound, in alignment
300 with predicted tissue tension (*73, 76*) (black lines, Fig. 5H). Mechanically bending, stretching,
301 restraining or compressing tissue also promotes alignments along the orientation of increased tissue
302 tension (*73, 77-80*). These observations support the hypothesis that the orientation of maximal
303 tissue tension can be sensed by cells to orient microtubules (*74*). Additionally, the cellulose synthesis
304 inhibitor isoxaben alters microtubule alignments, which has been taken to support the notion that
305 wall weakening leads to altered stress patterns (*81, 82*). However, the mechanism for sensing
306 maximal wall-stress orientation remains speculative (*74*).

307 Another explanation may be offered for the correlation between tissue stress and microtubule
308 orientation. Circumferential reorientation of microtubules after tissue damage may be a response

309 that evolved to mechanically reinforce cells at the wound site, mediated by chemical signalling and
310 cell polarity. For example, suppose cells contain two types of polarity protein, red and blue, that
311 localize at opposite cell ends. If a wound-induced chemical signal causes the red polarity proteins to
312 be activated in the plasma membrane adjacent to the wound site, polarity proteins in cells directly
313 bordering the wound would localize to cell faces oriented circumferentially around the wound (Fig.
314 5H). This polarity pattern could propagate further out to surrounding cells (darker grey) through cell-
315 cell signalling (*83*). If red and blue polarity proteins destabilize microtubules, microtubules would
316 become oriented circumferentially around the wound as this orientation would increase microtubule
317 survival probability. This hypothesis is consistent with induced pattern of cell polarity markers, which
318 either face towards or away from the wound site (*56, 82*). Disruption of auxin dynamics does not
319 prevent damage-induced cell polarity (*82*), indicating that polarity signalling is not auxin dependent.

320 Double ablation experiments, with an intact cell between two ablated cells (cyan, Fig. 5I), were
321 originally thought to preclude polarity as a microtubule-orienting mechanism because the cell
322 bridging the two ablations shows circumferential microtubule orientations, even though that cell has
323 no polarity (*73*). However, red polarity proteins could still be activated in the wound-facing plasma
324 membranes of the bridging cell, destabilizing microtubules and thus orienting microtubules in the
325 bridging cell parallel to its two red faces. Whether polarity proteins are localized in this manner for
326 double ablations remains to be tested. Cell polarity in shoot apices, may similarly provide the cue for
327 orienting microtubules.

328 The effects of mechanical manipulations (bending/compressing of tissue), and of isoxaben
329 treatment, may also have explanations that do not depend on stress sensing. Mechanical
330 manipulations cause cells to be stretched in the direction of maximal tension, changing cell
331 geometry. Such changes in geometry can modify microtubule orientations (*50*), potentially
332 accounting for the effects of mechanical manipulations on microtubule patterns. Changes in cell
333 geometry may be viewed as in indirect form of stress sensing in the case of mechanical
334 manipulations. However, changes in cell geometry cannot be used as a general mechanism to infer
335 stresses in growing plant cells. For example, in an axially-growing cylindrical cell, the cell elongates
336 axially, but wall stress is maximal circumferentially.

337 Isoxaben depletes cellulose synthase complexes from the plasma membrane. As these complexes
338 are tethered to microtubules, their depletion may affect microtubules directly, rather than via
339 weakening of walls (*54*). Cellulase treatment, which weakens the wall without targeting the cellulose
340 synthase complex, does not influence microtubule patterning (*54*). Similarly, mutants that reduce
341 the amount of cellulose without impairing cellulose-synthase tethering to microtubules have little
342 effect on microtubule patterns (*55*).

343 Thus, while wall-stress sensing is often invoked to explain microtubule orientations, the mechano-
344 sensing mechanisms remain elusive and the results may be accounted for by alternative mechanisms
345 based on chemical signalling and cell geometry.

346 Stresses have also been proposed to play a role in orienting cell polarity (*82*). According to this view,
347 stresses orient microtubules along the axis of maximal tension and orient cell polarity through stress
348 gradients. However, spherical protoplasts can become polarized in the absence of mechanical
349 asymmetries, showing that stress gradients are not needed for polarization (*63*). Thus, the role of
350 stresses versus chemical signals in the control of growth/microtubule orientation and polarity
351 remains controversial.

Tissue Patterning and Morphogenesis

Tissue morphogenesis depends on coupling the growth properties of walls, cells and tissues to regional patterning. Coupling may occur by regional gene activity that modifies rates of microfibril deposition and/or wall extensibility and yield thresholds, and thus wall growth via creep. Regional gene activity may also provide tissue cues that orient microtubule alignments, and thus the orientations of growth anisotropy.

Computational modelling, informed by developmental genetics, live imaging and growth analysis, has been used to determine whether such principles could account for tissue morphogenesis. From a modelling perspective we may distinguish between two types of growth (*84*). *Specified growth* is how a small region of tissue would grow in isolation and therefore free from tissue stresses. *Resultant growth* is the way a small region grows when mechanically connected to the rest of the tissue. Computational models allow resultant growth, and thus tissue deformation, to be calculated from an input pattern of specified growth rates and orientations. As tissue deforms, so do the regional patterns that determine the rates and orientations of specified growth, creating a feedback loop. If cell divisions are incorporated, they are typically based on division rules and are a consequence rather than cause of growth (*85-87*). Such a view follows naturally from plant growth mechanics, where growth rates depend on turgor, wall extensibility and yield thresholds, rather than introduction of new walls, which act mechanically to restrain rather than promote growth.

Models based on regionally-varying isotropic specified growth rates can account for the formation of bulges on the flanks of an apex, simulating early development of lateral appendages (primordia) (*88*). However, to account for more complex morphogenetic events, tissue-wide cues are needed to orient anisotropic specified growth. Use of tissue stresses to orient growth is problematic: if regions are reinforced in the direction of maximal stress, growth will be retarded in that direction, thwarting coherent changes in tissue shape (*84, 89*). Tissue-stress sensing may reinforce a shape, such as leaf flatness (*90*), but generating a new tissue shape is more difficult. To circumvent this problem, it has been proposed that global stresses across the developing organ may be sensed (*89*), though how global and local stresses might be discriminated by cells remains unclear.

The stress-feedback problem does not apply when polarity controlled by chemical cues (*83*) is used to orient specified growth. Although tissue-wide stresses are generated through differential growth (because of tissue connectivity), they do not disrupt growth-orienting polarity fields. Moreover, tissue-wide polarity fields have been described for several polarity proteins (*91*). Formation of flattened structures, like leaves, can be modelled with two orthogonal polarity fields, which act in combination to orient regionally-varying specified growth rates (*92, 93*). Leaf formation involves anisotropic growth oriented by a polarity field pointing from the tissue surface towards the ad-abaxial boundary (orthoplanar field). Orienting growth in this manner generates an initial primordial bulge followed by development of an extended flat or curved sheet. Growth and shaping of the sheet is oriented by a second (planar) polarity field (*93, 94*) (Fig. 6E). Modulation of planar polarity and growth rates at the leaf margins can generate serrated forms (*95*). Thus, regional variation in specified growth rates, oriented by tissue-wide polarity fields, can account for a range of plant morphogenetic behaviors.

Growth Arrest

Tissue growth slows down and finally arrests as plant cells mature and differentiate. Growth typically does not stop abruptly following cessation of cell division, but continues for a period, leading to cell enlargement. Growth arrest may eventually occur throughout a tissue, as with determinate organs such as leaves, or may be restricted to regions displaced away from meristems, as in stems or roots.

397 For determinate structures, such as leaves, sepals and the apical hook of seedlings, growth rates
398 decline gradually with time in a defined spatial pattern (*89, 94, 96-98*). This decline could arise
399 through reduced wall extensibility, increase in yield threshold, increase in wall thickness and/or
400 reduced turgor, but the contribution of each mechanism, and thus the control of final organ size,
401 remains unclear.

402 Conclusion

403 We have reviewed the mechanics of plant morphogenesis at different inter-related levels, from fiber
404 (Fig. 6 A and B), wall (Fig. 6 B and C), cell (Fig. 6 C and D) to tissue (Fig. 6 D and E). In moving up
405 levels, a population of components is typically abstracted to a continuum at the next level (e.g. fibers
406 to wall, walls to cell, cells to tissue). These abstractions help to both clarify concepts and simplify
407 simulations. Mechanical stresses operate at each level, but values are typically not the same from
408 one level to the next. Viewing the levels together, the cellulose network at the fiber/wall level
409 provides elastic resistance to deformation while allowing growth through creep, enabling
410 morphogenesis at the cell/tissue level, while maintaining mechanical strength.

411 A key question is how patterns of gene expression at the tissue level modify behaviors and
412 mechanics at other levels to generate tissue morphogenesis. Although we have outlined broad
413 principles for how this may operate, many of the underlying molecular mechanisms are unresolved.
414 Controversies remain over the role of pectins in controlling wall mechanics, and over the role of
415 mechanosensing or chemical signalling in controlling orientations of growth. And although tissue-
416 level models have been proposed to account for morphogenetic changes (e.g. Fig. 6E), many of the
417 underlying components remain hypothetical. A further challenge is to determine how interactions
418 across levels have been modified during evolution to give rise to the diversity of plant forms (*99*).

419 To what extent can the principles of plant morphogenesis be extended to microbial and animal
420 development? Like plants, bacteria and fungi have cell walls with fibers that confer mechanical
421 strength, but correspond to peptidoglycans, glycans or chitin rather than cellulose (*100, 101*).
422 Growth depends on turgor, though the extent to which turgor and/or insertion of new wall material
423 drives growth remains to be clarified (*102*). Animal cells have a network of fibers, the actin cortex,
424 that lies immediately beneath the plasma membrane and plays a comparable role to a cell wall in
425 mechanics: conferring mechanical stiffness, and resistance to external mechanical stresses and
426 turgor (*103, 104*). Sliding of these fibers likely plays a key role in animal morphogenesis, but unlike
427 plants, can be active (e.g. contractile) as well as passive (caused by turgor or tissue stresses). Animal
428 cells can rearrange and migrate during morphogenesis, but the extent of rearrangement is limited
429 for many growing tissues, evidenced by coherence of clonal sectors (*105-107*). Thus, organogenesis
430 presents similar issues for coordination of growth/division orientation as in plants, such as the role
431 of polarity and stresses (*108*). Animal morphogenesis is also influenced mechanically and chemically
432 by the extracellular matrix, which contains fibers, such as collagen, that may slide past each other to
433 stretch irreversibly (*109, 110*). Thus, although the molecular players and interactions are different,
434 many of the mechanical principles and issues outlined in this review may also be applicable to
435 microbial and animal morphogenesis.

436

437 References

438 1. A. N. J. Heyn, The physiology of cell elongation. *Bot Rev* **6**, 515-574 (1940).
439 2. J. A. Lockhart, An analysis of irreversible plant cell elongation. *J Theor Biol* **8**, 264-275 (1965).
440 3. P. B. Green, R. O. Erickson, J. Buggy, Metabolic and physical control of cell elongation rate: in
441 vivo studies in *Nitella*. *Plant Physiology* **47**, 423-430 (1971).
442 4. K. T. Haas, R. Wightman, E. M. Meyerowitz, A. Peaucelle, Pectin homogalacturonan
443 nanofilament expansion drives morphogenesis in plant epidermal cells. *Science* **367**, 1003-
444 1007 (2020).
445 5. A. Ursprung, G. Blum, Eine Methode zur Messung des Wandund Turgordruckes der Zelle
446 nebst Anwendungen. *Jahrb. Wiss. Bot.* **63**, 1-110 (1924).
447 6. D. J. Cosgrove, C. T. Anderson, Plant Cell Growth: Do Pectins Drive Lobe Formation in
448 Arabidopsis Pavement Cells? *Curr Biol* **30**, R660-R662 (2020).
449 7. M. C. Jarvis, Structure of native cellulose microfibrils, the starting point for nanocellulose
450 manufacture. *Philos Trans A Math Phys Eng Sci* **376**, 20170045 (2018).
451 8. Y. Zhang *et al.*, Molecular insights into the complex mechanics of plant epidermal cell walls.
452 *Science* **372**, 706-711 (2021).
453 9. D. J. Cosgrove, Catalysts of plant cell wall loosening. *F1000Res* **5**, Doi
454 10.12688/f11000research.17180.12681 (2016).
455 10. T. Zhang, D. Vavylonis, D. M. Durachko, D. J. Cosgrove, Nanoscale movements of cellulose
456 microfibrils in primary cell walls. *Nature Plants* **3**, 17056 (2017).
457 11. W. J. Nicolas *et al.*, Cryo-electron tomography of the onion cell wall shows bimodally
458 oriented cellulose fibers and reticulated homogalacturonan networks. *Curr Biol* **32**, 2375-
459 2389 e2376 (2022).
460 12. D. J. Cosgrove, Building an extensible cell wall. *Plant Physiology* **189**, 1246-1277 (2022).
461 13. A. M. Saffer, Expanding roles for pectins in plant development. *J Integr Plant Biol* **60**, 910-
462 923 (2018).
463 14. K. T. Haas, R. Wightman, A. Peaucelle, H. Hofte, The role of pectin phase separation in plant
464 cell wall assembly and growth. *Cell Surf* **7**, 100054 (2021).
465 15. A. J. Bidhendi, A. Geitmann, Relating the mechanics of the primary plant cell wall to
466 morphogenesis. *J Exp Bot* **67**, 449-461 (2016).
467 16. T. Zhang, H. Tang, D. Vavylonis, D. J. Cosgrove, Disentangling loosening from softening:
468 insights into primary cell wall structure. *Plant Journal* **100**, 1101-1117 (2019).
469 17. M. C. Jarvis, Control of thickness of collenchyma cell walls by pectins. *Planta* **187**, 218-220
470 (1992).
471 18. J. Du, C. T. Anderson, C. Xiao, Dynamics of pectic homogalacturonan in cellular
472 morphogenesis and adhesion, wall integrity sensing and plant development. *Nature Plants* **8**,
473 332-340 (2022).
474 19. K. Jonsson, O. Hamant, R. P. Bhalerao, Plant cell walls as mechanical signaling hubs for
475 morphogenesis. *Curr Biol* **32**, R334-R340 (2022).
476 20. Z. L. Yue *et al.*, The receptor kinase OsWAK11 monitors cell wall pectin changes to fine-tune
477 brassinosteroid signaling and regulate cell elongation in rice. *Curr Biol* **32**, 2454-2466 e2457
478 (2022).
479 21. G. Levesque-Tremblay, J. Pelloux, S. A. Braybrook, K. Muller, Tuning of pectin
480 methylesterification: consequences for cell wall biomechanics and development. *Planta* **242**,
481 791-811 (2015).
482 22. S. A. Braybrook, A. Peaucelle, Mechano-chemical aspects of organ formation in *Arabidopsis*
483 *thaliana*: the relationship between auxin and pectin. *PloS one* **8**, e57813 (2013).
484 23. F. Bou Daher *et al.*, Anisotropic growth is achieved through the additive mechanical effect of
485 material anisotropy and elastic asymmetry. *eLife* **7**, e38161 (2018).
486 24. A. Peaucelle, R. Wightman, H. Hofte, The control of growth symmetry breaking in the
487 arabidopsis hypocotyl. *Curr Biol* **25**, 1746-1752 (2015).

25. M. C. Jarvis, Hydrogen bonding and other non-covalent interactions at the surfaces of cellulose microfibrils. *Cellulose*, (2022).
26. Y. B. Park, D. J. Cosgrove, A revised architecture of primary cell walls based on biomechanical changes induced by substrate-specific endoglucanases. *Plant Physiology* **158**, 1933-1943 (2012).
27. D. J. Cosgrove, Relaxation in a high-stress environment: The molecular bases of extensible cell walls and cell enlargement. *Plant Cell* **9**, 1031-1041 (1997).
28. K. Takahashi, S. Hirata, N. Kido, K. Katou, Wall-yielding properties of cell walls from elongating cucumber hypocotyls in relation to the action of expansin. *Plant and Cell Physiology* **47**, 1520-1529 (2006).
29. W. Lin *et al.*, TMK-based cell-surface auxin signalling activates cell-wall acidification. *Nature* **599**, 278-282 (2021).
30. K. Nakahori, K. Katou, H. Okamoto, Auxin changes both the extensibility and the yield threshold of the cell wall of *Vigna* hypocotyls. *Plant and Cell Physiology* **32**, 121-129 (1991).
31. B. Moulia, Plant biomechanics and mechanobiology are convergent paths to flourishing interdisciplinary research. *J Exp Bot* **64**, 4617-4633 (2013).
32. T. W. Wang, D. J. Cosgrove, R. N. Arteca, Brassinosteroid Stimulation of Hypocotyl Elongation and Wall Relaxation in Pakchoi (*Brassica chinensis* cv Lei-Choi). *Plant Physiology* **101**, 965-968 (1993).
33. G. Refregier, S. Pelletier, D. Jaillard, H. Hofte, Interaction between wall deposition and cell elongation in dark-grown hypocotyl cells in Arabidopsis. *Plant Physiology* **135**, 959-968 (2004).
34. J. Verbancic, J. E. Lunn, M. Stitt, S. Persson, Carbon Supply and the Regulation of Cell Wall Synthesis. *Mol Plant* **11**, 75-94 (2018).
35. H. Edelmann, R. Bergfeld, P. Schopfer, Role of cell-wall biogenesis in the initiation of auxin-mediated growth in coleoptiles of Zea mays L. *Planta* **179**, 486-494 (1989).
36. P. B. Green, The spiral growth pattern of the cell wall in *Nitella axillaris*. *Am J Bot* **41**, 403-409 (1954).
37. P. A. Richmond, Patterns of Cellulose Microfibril Deposition and Rearrangement in *Nitella*: in vivo Analysis by a Birefringence Index. *Journal of Applied Polymer Science* **37**, 107-122 (1983).
38. A. J. Bidhendi, A. Geitmann, Finite Element Modeling of Shape Changes in Plant Cells. *Plant Physiology* **176**, 41-56 (2018).
39. A. J. Bidhendi, B. Altartouri, F. P. Gosselin, A. Geitmann, Mechanical Stress Initiates and Sustains the Morphogenesis of Wavy Leaf Epidermal Cells. *Cell Reports* **28**, 1237-1250.e1236 (2019).
40. E. S. Castle, Membrane tension and orientation of structure in the plant cell wall. *Journal of Cellular and Comparative Physiology* **10**, 113-121 (1937).
41. C. M. Rounds, M. Bezanilla, Growth mechanisms in tip-growing plant cells. *Annu Rev Plant Biol* **64**, 243-265 (2013).
42. D. J. Cosgrove, Diffuse growth of plant cell walls. *Plant Physiology* **176**, 16-27 (2018).
43. P. B. Green, Mechanism for plant cellular morphogenesis. *Science* **138**, 1404-& (1962).
44. J. P. Metraux, L. Taiz, Transverse viscoelastic extension in *Nitella*: I. Relationship to growth rate. *Plant Physiology* **61**, 135-138 (1978).
45. A. R. Paredez, C. R. Somerville, D. W. Ehrhardt, Visualization of cellulose synthase demonstrates functional association with microtubules. *Science* **312**, 1491-1495 (2006).
46. J. Chan, E. Coen, Interaction between Autonomous and Microtubule Guidance Systems Controls Cellulose Synthase Trajectories. *Curr Biol* **30**, 941-947 e942 (2020).
47. R. Dixit, R. Cyr, Encounters between dynamic cortical microtubules promote ordering of the cortical array through angle-dependent modifications of microtubule behavior. *Plant Cell* **16**, 3274-3284 (2004).

539 48. B. Chakrabortty, I. Blilou, B. Scheres, B. M. Mulder, A computational framework for cortical
540 microtubule dynamics in realistically shaped plant cells. *PLoS Comput Biol* **14**, e1005959
541 (2018).
542 49. S. H. Tindemans, R. J. Hawkins, B. M. Mulder, Survival of the aligned: ordering of the plant
543 cortical microtubule array. *Phys Rev Lett* **104**, 058103 (2010).
544 50. P. Durand-Smet, T. A. Spelman, E. M. Meyerowitz, H. Jonsson, Cytoskeletal organization in
545 isolated plant cells under geometry control. *Proc Natl Acad Sci U S A* **117**, 17399-17408
546 (2020).
547 51. L. Colin *et al.*, Cortical tension overrides geometrical cues to orient microtubules in confined
548 protoplasts. *Proc Natl Acad Sci U S A* **117**, 32731 (2020).
549 52. P. B. Green, A. King, A mechanism for the origin of specifically oriented textures in
550 development with special reference to *Nitella* wall texture. *Aust J Biol Sci* **19**, 421-437 (1966).
551 53. R. E. Williamson, Alignment of Cortical Microtubules by Anisotropic Wall Stresses. *Aust J*
552 *Plant Physiol* **17**, 601-613 (1990).
553 54. A. R. Paredez, S. Persson, D. W. Ehrhardt, C. R. Somerville, Genetic evidence that cellulose
554 synthase activity influences microtubule cortical array organization. *Plant Physiology* **147**,
555 1723-1734 (2008).
556 55. R. Schneider, D. W. Ehrhardt, E. M. Meyerowitz, A. Sampathkumar Tethering of cellulose
557 synthase to microtubules dampens mechano-induced cytoskeletal organization in
558 Arabidopsis pavement cells. *Nature Plants* **8**, 1064-1073 (2022).
559 56. M. Bringmann, D. C. Bergmann, Tissue-wide Mechanical Forces Influence the Polarity of
560 Stomatal Stem Cells in Arabidopsis. *Curr Biol* **27**, 877-883 (2017).
561 57. P. Krecek *et al.*, The PIN-FORMED (PIN) protein family of auxin transporters. *Genome Biol* **10**,
562 249 (2009).
563 58. J. Dong, C. A. MacAlister, D. C. Bergmann, BASL controls asymmetric cell division in
564 Arabidopsis. *Cell* **137**, 1320-1330 (2009).
565 59. E. Truernit *et al.*, High-resolution whole-mount imaging of three-dimensional tissue
566 organization and gene expression enables the study of Phloem development and structure
567 in Arabidopsis. *Plant Cell* **20**, 1494-1503 (2008).
568 60. S. Yoshida *et al.*, A SOSEKI-based coordinate system interprets global polarity cues in
569 Arabidopsis. *Nat Plants* **5**, 160-166 (2019).
570 61. L. J. Pillitteri, K. M. Peterson, R. J. Horst, K. U. Torii, Molecular profiling of stomatal
571 meristemoids reveals new component of asymmetric cell division and commonalities among
572 stem cell populations in Arabidopsis. *Plant Cell* **23**, 3260-3275 (2011).
573 62. E. Truernit, H. Bauby, K. Belcram, J. Barthelemy, J. C. Palauqui, OCTOPUS, a polarly localised
574 membrane-associated protein, regulates phloem differentiation entry in Arabidopsis
575 thaliana. *Development* **139**, 1306-1315 (2012).
576 63. J. Chan, C. Mansfield, F. Clouet, D. Dorussen, E. Coen, Intrinsic Cell Polarity Coupled to
577 Growth Axis Formation in Tobacco BY-2 Cells. *Curr Biol* **30**, 4999-5006 e4993 (2020).
578 64. C. Ambrose, J. F. Allard, E. N. Cytrynbaum, G. O. Wasteneys, A CLASP-modulated cell edge
579 barrier mechanism drives cell-wide cortical microtubule organization in Arabidopsis. *Nat*
580 *Commun* **2**, 430 (2011).
581 65. S. Liu, F. Jobert, Z. Rahneshan, S. M. Doyle, S. Robert, Solving the Puzzle of Shape Regulation
582 in Plant Epidermal Pavement Cells. *Annu Rev Plant Biol* **72**, 525-550 (2021).
583 66. F. B. Daher, S. A. Braybrook, How to let go: pectin and plant cell adhesion. *Front Plant Sci* **6**,
584 523 (2015).
585 67. W. S. Peters, A. D. Tomos, The history of tissue tension. *Ann Bot* **77**, 657-665 (1996).
586 68. S. Verger, Y. Long, A. Boudaoud, O. Hamant, A tension-adhesion feedback loop in plant
587 epidermis. *eLife* **7**, (2018).
588 69. U. Kutschera, K. J. Niklas, The epidermal-growth-control theory of stem elongation: an old
589 and a new perspective. *J Plant Physiol* **164**, 1395-1409 (2007).

70. Z. Hejnowicz, A. Sievers, Tissue stresses in organs of herbaceous plants II. Determination in three dimensions in the hypocotyl of sunflower. *J Exp Bot* **46**, 1045-1053 (1995).
71. Z. Hejnowicz, A. Sievers, Tissue stresses in organs of herbaceous plants I. Poisson ratios of tissues and their role in determination of the stresses. *J Exp Bot* **289**, 1035-1043 (1995).
72. A. Goriely, *The Mathematics and Mechanics of Biological Growth*. (Springer, New York, 2017).
73. O. Hamant *et al.*, Developmental patterning by mechanical signals in Arabidopsis. *Science* **322**, 1650-1655 (2008).
74. O. Hamant, D. Inoue, D. Bouchez, J. Dumais, E. Mjolsness, Are microtubules tension sensors? *Nat Commun* **10**, 2360 (2019).
75. M. G. Heisler, Integration of Core Mechanisms Underlying Plant Aerial Architecture. *Front Plant Sci* **12**, 786338 (2021).
76. J. M. Hush, C. R. Hawes, R. L. Overall, Interphase microtubule re-orientation predicts a new cell polarity in wounded pea roots. *Journal of Cell Science* **96**, 47-61 (1990).
77. Z. Hejnowicz, A. Rusin, T. Rusin, Tensile tissue stress affects the orientation of cortical microtubules in the epidermis of sunflower hypocotyl. *J Plant Growth Regul* **19**, 31-44 (2000).
78. A. Burian, Z. Hejnowicz, Strain rate does not affect cortical microtubule orientation in the isolated epidermis of sunflower hypocotyls. *Plant Biology* **12**, 459-468 (2009).
79. S. Robinson, C. Kuhlemeier, Global Compression Reorients Cortical Microtubules in Arabidopsis Hypocotyl Epidermis and Promotes Growth. *Curr Biol* **28**, 1794-1802 e1792 (2018).
80. K. Zandomeni, P. Schopfer, Mechanosensory microtubule reorientation in the epidermis of maize coleoptiles subjected to bending stress. *Protoplasma* **182**, 96-101 (1994).
81. D. D. Fisher, R. J. Cyr, Extending the Microtubule/Microfibril paradigm. Cellulose synthesis is required for normal cortical microtubule alignment in elongating cells. *Plant Physiology* **116**, 1043-1051 (1998).
82. M. G. Heisler *et al.*, Alignment between PIN1 polarity and microtubule orientation in the shoot apical meristem reveals a tight coupling between morphogenesis and auxin transport. *PLoS Biol* **8**, e1000516 (2010).
83. K. Abley *et al.*, An intracellular partitioning-based framework for tissue cell polarity in plants and animals. *Development* **140**, 2061-2074 (2013).
84. E. Coen, R. Kennaway, C. Whitewoods, On genes and form. *Development* **144**, 4203-4213 (2017).
85. L. Errera, Sur une condition fondamentale d'équilibre des cellules vivantes. *C.R. Acad. Sci.* **103**, 822-824 (1886).
86. P. Prusinkiewicz, A. Runions, Computational models of plant development and form. *New Phytol* **193**, 549-569 (2012).
87. S. Yoshida *et al.*, Genetic control of plant development by overriding a geometric division rule. *Developmental Cell* **29**, 75-87 (2014).
88. F. Boudon *et al.*, A computational framework for 3D mechanical modeling of plant morphogenesis with cellular resolution. *PLoS Comput Biol* **11**, e1003950 (2015).
89. N. Hervieux *et al.*, A Mechanical Feedback Restricts Sepal Growth and Shape in Arabidopsis. *Curr Biol* **26**, 1019-1028 (2016).
90. F. Zhao *et al.*, Microtubule-Mediated Wall Anisotropy Contributes to Leaf Blade Flattening. *Curr Biol* **30**, 3972-3985 e3976 (2020).
91. V. Gorelova, J. Sprakel, D. Weijers, Plant cell polarity as the nexus of tissue mechanics and morphogenesis. *Nat Plants* **7**, 1548-1559 (2021).
92. C. D. Whitewoods *et al.*, Evolution of carnivorous traps from planar leaves through simple shifts in gene expression. *Science* **367**, 91-96 (2020).

93. A. E. Richardson *et al.*, Evolution of the grass leaf by primordium extension and petiole-lamina remodeling. *Science* **374**, 1377-1381 (2021).
94. S. Fox *et al.*, Spatiotemporal coordination of cell division and growth during organ morphogenesis. *PLoS Biol* **16**, e2005952 (2018).
95. D. Kierzkowski *et al.*, A Growth-Based Framework for Leaf Shape Development and Diversity. *Cell* **177**, 1405-1418 e1417 (2019).
96. M. Zhu *et al.*, Robust organ size requires robust timing of initiation orchestrated by focused auxin and cytokinin signalling. *Nat Plants* **6**, 686-698 (2020).
97. P. Zadnikova *et al.*, A Model of Differential Growth-Guided Apical Hook Formation in Plants. *Plant Cell* **28**, 2464-2477 (2016).
98. Q. Zhu, P. Žádníková, D. Smet, D. Van Der Straeten, E. Benková, Real-Time Analysis of the Apical Hook Development. *Methods in Molecular Biology* **1497**, 1-8 (2017).
99. D. Wilson-Sanchez, N. Bhatia, A. Runions, M. Tsiantis, From genes to shape in leaf development and evolution. *Curr Biol* **32**, R1215-R1222 (2022).
100. N. A. R. Gow, M. D. Lenardon, Architecture of the dynamic fungal cell wall. *Nat Rev Microbiol* **online before print** https://doi.org/10.1038/s41579-022-00796-9, (2022).
101. T. Dorr, P. J. Moynihan, C. Mayer, Editorial: Bacterial Cell Wall Structure and Dynamics. *Front Microbiol* **10**, 2051 (2019).
102. E. R. Rojas, K. C. Huang, Regulation of microbial growth by turgor pressure. *Curr Opin Microbiol* **42**, 62-70 (2018).
103. G. Salbreux, G. Charras, E. Paluch, Actin cortex mechanics and cellular morphogenesis. *Trends Cell Biol* **22**, 536-545 (2012).
104. T. Kim, M. L. Gardel, E. Munro, Determinants of fluidlike behavior and effective viscosity in cross-linked actin networks. *Biophys J* **106**, 526-534 (2014).
105. L. Marcon, C. G. Arques, M. S. Torres, J. Sharpe, A computational clonal analysis of the developing mouse limb bud. *PLoS Comput Biol* **7**, e1001071 (2011).
106. S. M. Meilhac *et al.*, A retrospective clonal analysis of the myocardium reveals two phases of clonal growth in the developing mouse heart. *Development* **130**, 3877-3889 (2003).
107. F. Germani, C. Bergantinos, L. A. Johnston, Mosaic Analysis in *Drosophila*. *Genetics* **208**, 473-490 (2018).
108. L. LeGoff, T. Lecuit, Mechanical Forces and Growth in Animal Tissues. *Cold Spring Harb Perspect Biol* **8**, a019232 (2015).
109. B. Sun, The mechanics of fibrillar collagen extracellular matrix. *Cell Rep Phys Sci* **2**, (2021).
110. M. L. Wood, G. E. Lester, L. E. Dahners, Collagen fiber sliding during ligament growth and contracture. *J Orthop Res* **16**, 438-440 (1998).

Acknowledgements

We would like to thank Phil Robinson for filming/editing the movies, Jordi Chan, Pauline Durand-Smet, Anna Hanner, Richard Kennaway, Richard Smith and Sulin Zhang for helpful comments on the manuscript. **Funding:** We acknowledge support from HFSP for a collaborative research grant RGP0005/2022 awarded to the authors of this review. EC was supported by grants from the UK Biotechnology and Biological Sciences Research Council (BB/M023117/1, BB/W007924/1, BBS/E/J/000PR9787, BBS/E/J/00000152, BB/L008920/1, BBS/E/J/000PR9789). DJC was supported by the US Department of Energy under Awards #DE-SC0001090 for work on wall structure and #DE-FG2-84ER13179 for work on expansins and wall mechanics. **Competing interests:** The authors have no competing interests. **Open access:** For the purpose of open access, the authors have applied a Creative Commons Attribution (CC BY) to the Accepted Manuscript.

Figures and Legends

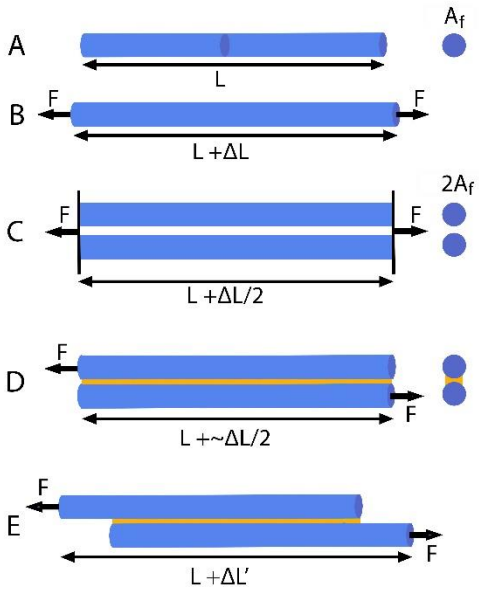

Fig. 1 Fiber growth in one dimension.
A Fiber of length L and cross-sectional area A_f. **B** Tensile force, F, leads to extension ΔL. Strain $\varepsilon_f = \Delta L/L$. For an idealized linear elastic fiber, $\varepsilon_f = \sigma_f / E_f$, where σ_f is the fiber tensile stress F/A_f, and E_f is the Young's modulus of the fiber. **C** Doubling fiber number halves stress and strain. **D** Shear stress, τ_f, generated at fiber interface (yellow), equals F/A_c, where A_c is the contact area along the length of the fibers. If cross-sectional area of the interface is small relative to A_f, $\varepsilon_f \sim \Delta L/2L$. **E** Slippage caused by shear stress. Fiber extension $\Delta L'$ increases with time.

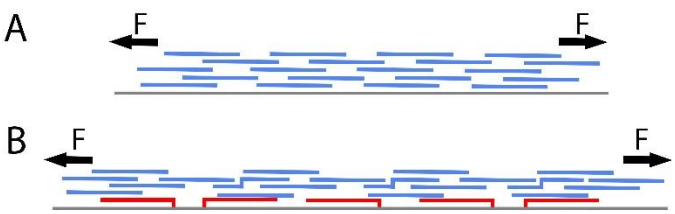

Fig. 2 Wall growth in one dimension.
Schematic of fibers in a wall cross-section with plasma membrane shown as grey line and newly deposited fibers in red. **A** Before growth. **B** After growth by fiber slippage, with newly deposited fibers (red) maintaining wall thickness.

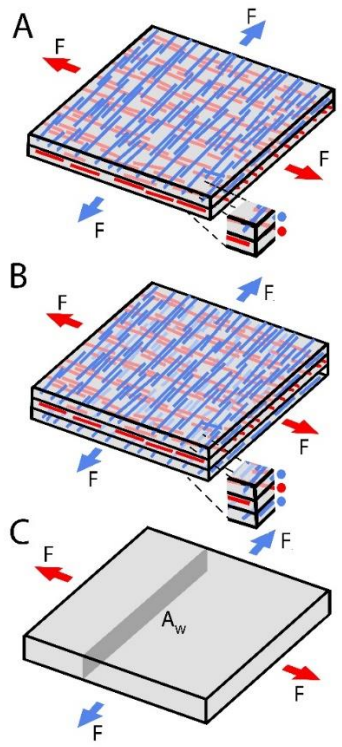

Fig. 3 Wall growth in two dimensions.
A Two layers of microfibrils, with equal number of microfibrils in red and blue orientations. **B** Three layers of microfibrils, with twice as many microfibrils in blue than red orientations. **C** Continuum perspective.

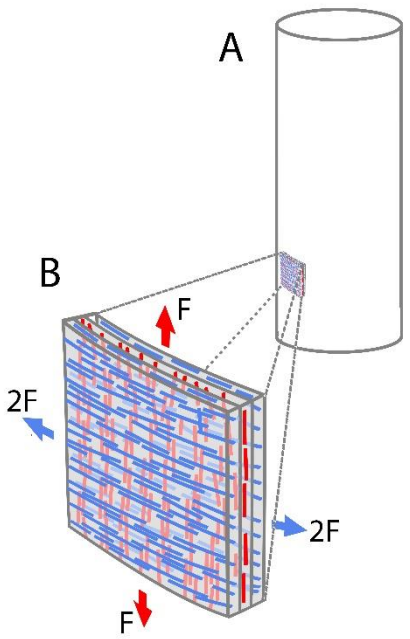

Fig. 4 Mechanics of a cylindrical cell.
A Cell outline. **B** Microfibril composition and tensile forces on a small region of anisotropic wall with two layers of circumferential microfibrils (blue) and one layer of axial microfibrils (red).

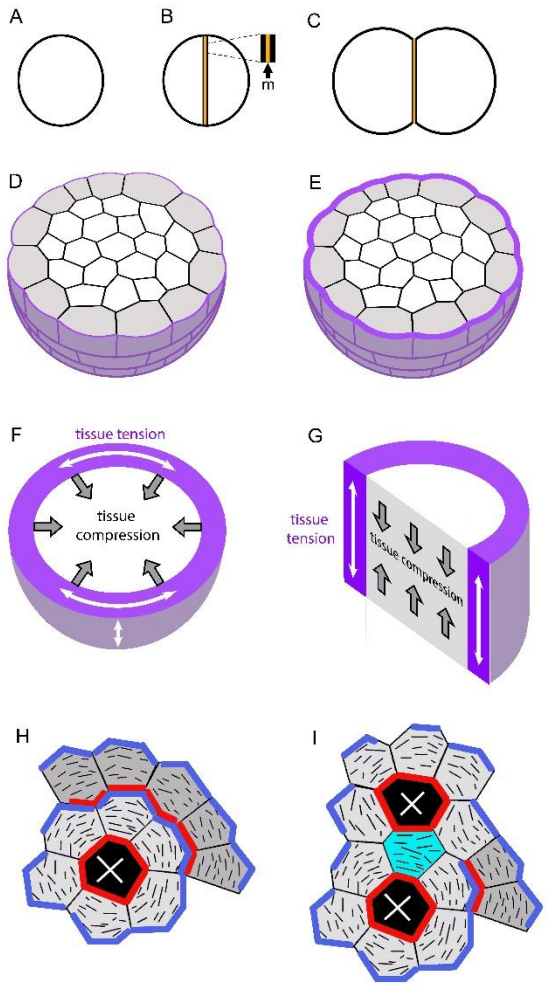

Fig. 5 Multicellular interactions.
Spherical cell (**A**) divides to give two daughters (**B**) separated by middle lamella (yellow, m). Isotropic growth and strong adhesion leads to formation of two cells with a flattened interface (**C**). **D** In a spherical tissue with isotropic walls of uniform width (shown in cross section), all walls experience similar tensile stress. Outer wall of epidermal cells (grey) shown in purple. **E** With thickened outer walls, growth leads to higher tensile force on the outer walls, corresponding to tissue tension in an outer region (purple) and tissue compression in the inner region of a continuous tissue (**F**). **G** With a cylindrical tissue that grows axially (half section shown), thickened outer walls leads to axial outer tissue tension and axial inner tissue compression. **H** With single cell ablation (black cell with cross), microtubules (black lines) become oriented circumferentially around the wound in cells directly bordering the wound (light grey) and cells further out (dark grey). This could be explained by circumferential stresses caused by the wound orienting microtubules. Alternatively, cells could have polarity proteins (red, blue) that localize at opposite cell ends. If red polarity proteins are activated adjacent to the wound by a chemical signal, polarity proteins in cells bordering the wound would localize to faces oriented circumferentially around the wound. This polarity pattern could propagate to further out (dark grey cells) through molecular signalling. Destabilization of microtubules by red and blue polarity proteins would favor microtubules orientations parallel to the red and blue faces (i.e. circumferential to the wound) as this increases microtubule survival probability. **I** In a double ablation, microtubules in the bridging cell (cyan) are oriented parallel to the wound cell faces, which could be explained by mechanosensing. Alternatively, red polarity proteins could be activated at both faces of the bridging cell adjacent to the wounds, destabilising microtubules and favouring microtubule orientations in the bridging cell parallel to its two red faces.

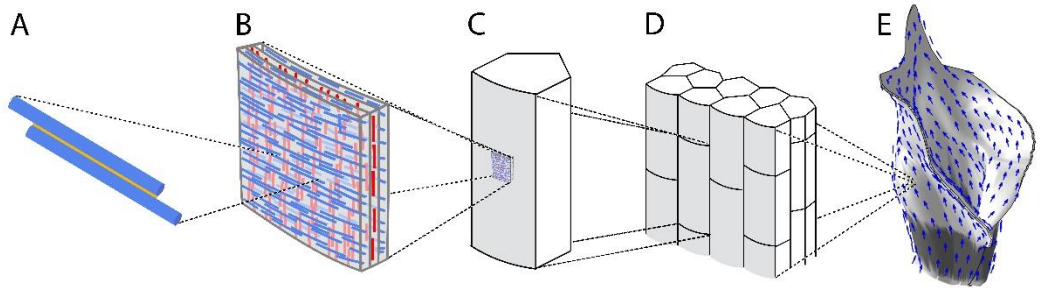

Fig. 6 Plant morphogenesis, from nano- to macroscale.
Growth begins with sliding of cellulose fibers **(A)** within the cohesive, extensible and structurally-biased networks of cell walls **(B)**. Sliding is physically driven by turgor pressure, which generates stress patterns in single cells **(C)** and across tissues **(D)**. Growth may be oriented by polarity fields (arrows) to generate complex forms, illustrated by a tissue-level model of grass leaf development **(E)**, with tubular sheath region in darker grey (*93*).

Movie Stills and Legends

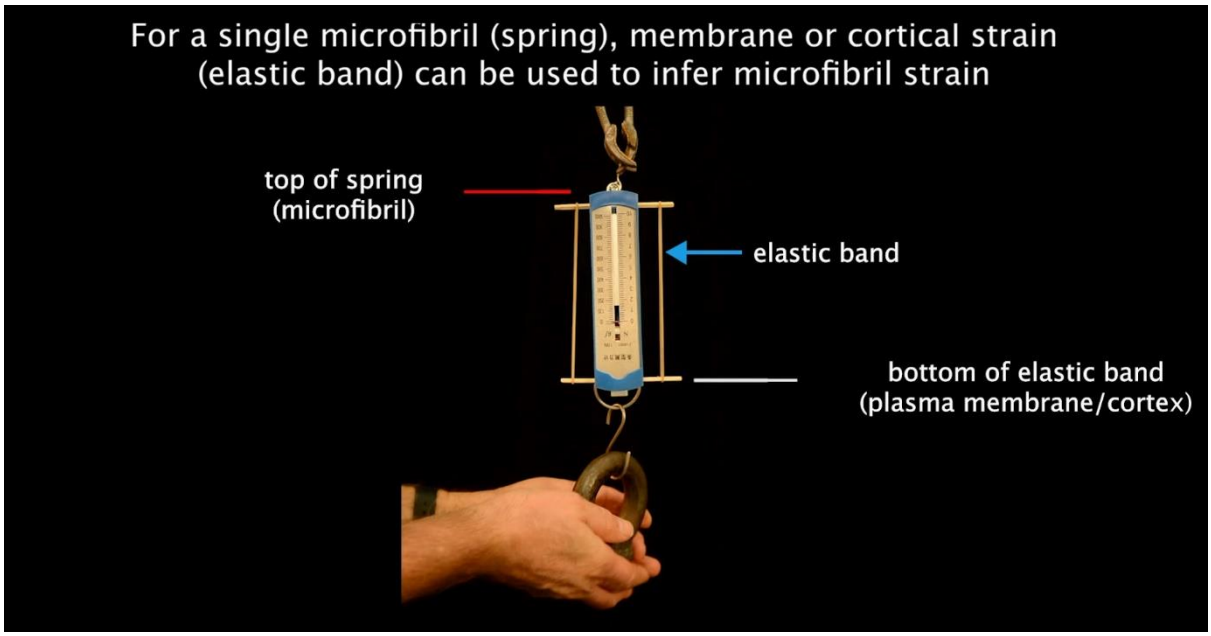

Movie 1 For a single microfibril (spring), membrane or cortical strain (elastic band) can be used to infer microfibril strain.
When a weight is applied, extension of a spring (equivalent to fiber in Fig. 1B) is the same as the extension of a less stiff elastic band attached to the spring.

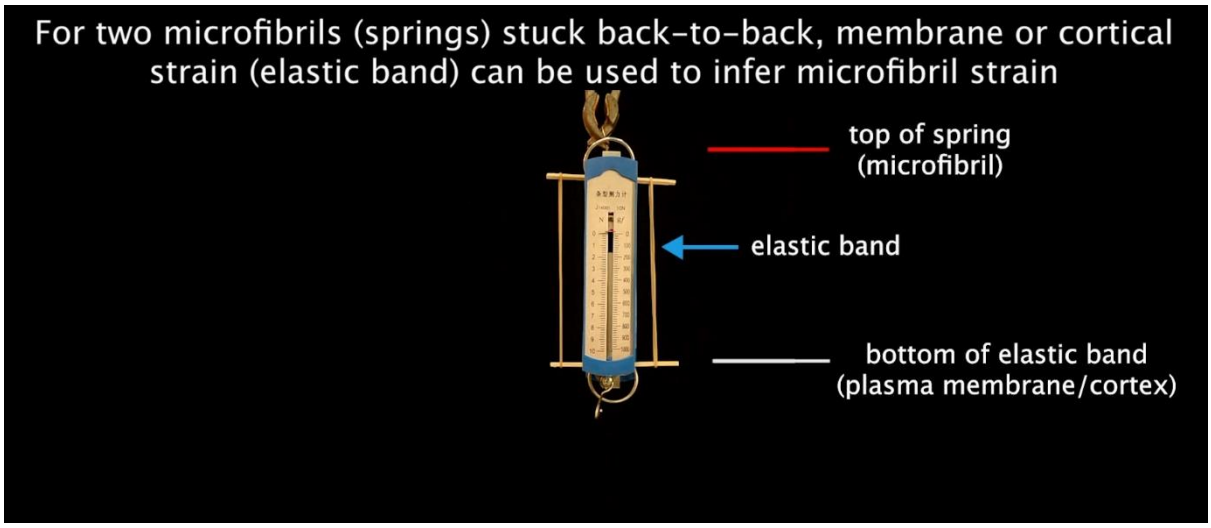

Movie 2 For two microfibrils (springs) stuck back-to-back, membrane or cortical strain (elastic band) can be used to infer microfibril strain.
When a weight is applied to two firmly attached springs, extension of the springs (equivalent to fibers in Fig. 1D), is the same as the extension of a less stiff elastic band attached to the springs.

Movie 3 For two microfibrils (springs) stuck loosely together, membrane or cortical strain (elastic band) cannot be used to infer microfibril strain.
When a weight is applied to two springs held together with honey, slippage (as in Fig. 1E) increases with time, and leads to greater strain for the elastic band than for the individual springs.

764 # Print page summary

765 ## Background

766 The growth and shape of plants depend on the mechanical properties of the plant's mesh of
767 interconnected cell walls. Because adhering cell walls prevent cell migrations, morphogenesis is
768 simpler to study in plants than in animals. Spatiotemporal variations in the rates and orientations at
769 which cell walls yield to mechanical stresses – ultimately powered by cell turgor pressure – underlie
770 the development and diversity of plant forms. Here we review new insights and points of current
771 contention in our understanding of plant morphogenesis, starting from wall components and
772 building up to cells and tissues.

773 ## Advances

774 Recent modelling and experimental studies have enabled advances at four levels: fiber, wall, cell and
775 tissue. In moving up levels, a population of components is typically abstracted to a continuum at the
776 next level (e.g. fibers to wall, walls to cell, cells to tissue). These abstractions help to both clarify
777 concepts and simplify simulations. Mechanical stresses operate at each level, but values are typically
778 not the same from one level to the next.

779 At the fiber level, growth corresponds to cellulose microfibrils sliding past each other, passively
780 driven by turgor-induced tension. The rate of sliding depends on adhesion between microfibrils,
781 while anisotropy reflects differences in the proportion of fibers in different orientations. Growth
782 occurs preferentially in the direction of maximal microfibril stress.

783 At the wall level, microfibril sliding corresponds to cell wall creep, at rates dependent on turgor, wall
784 extensibility, thickness and yield thresholds. Anisotropic mechanical properties can arise through
785 orientation-selective synthesis of cellulose microfibrils, guided by microtubules. Creep is stimulated
786 by the wall-loosening action of expansins, which increase extensibility and lower the yield threshold.
787 Wall synthesis and loosening influence growth in complementary ways. Wall loosening increases
788 growth rate with almost immediate effect, but unless wall synthesis increases in parallel, wall
789 thickness declines over time, potentially weakening the wall. Wall synthesis requires a longer
790 timescale to have a discernible growth effect but is critical for maintaining wall thickness and
791 orienting anisotropy. By regulating loosening and synthesis separately, plants have the flexibility to
792 produce rapid growth responses as well as control longer term growth patterns and mechanical
793 strength.

794 At the cellular level, growth corresponds to irreversible deformations catalyzed by expansins and
795 physically driven by mechanical stresses arising from turgor acting on cell walls. Oriented cell growth
796 depends on wall anisotropy and cell geometry, which in turn depend on the dynamics of
797 microtubule alignment. Collisions between microtubules lead to self-organized alignments which
798 may be influenced by cellular cues and cell geometry.

799 At the tissue level, cell-cell adhesion combined with differential wall properties can lead to tissue-
800 wide stresses. Tissue morphogenesis depends on coupling the mechanical properties of walls, cells
801 and tissues to regional patterning. Coupling may occur by regional gene activity that modifies rates
802 of microfibril deposition, wall extensibility and/or yield thresholds, and thus wall growth via creep.
803 Regional gene activity may also provide tissue cues that orient microtubule alignments, and thus the
804 orientations of growth anisotropy. Computational modelling, informed by developmental genetics,
805 live imaging and growth analysis, has shown how these principles can account for morphogenetic

changes through mechanically connected tissue regions irreversibly growing at specified rates and orientations.

Taken as a whole, the cellulose network at the fiber/wall level provides elastic resistance to deformation while allowing growth through creep, enabling morphogenesis at the cell/tissue level, while maintaining mechanical strength.

Outlook

A key question is how patterns of gene expression at the tissue level modify behaviors and mechanics at other levels to generate tissue morphogenesis. Although we outline broad principles for how this may operate, many of the underlying molecular mechanisms remain unresolved. Controversies remain over the role of pectins in controlling wall mechanics and in the role of mechanosensing, chemical signalling and polarity in controlling orientations of growth. And although tissue-level models have been proposed to account for morphogenetic changes, many of the underlying components remain hypothetical. A further challenge is to determine how interactions across levels been modified during evolution to give rise to the diversity of plant forms.

Many of the principles described here may also be applicable to microbial and animal morphogenesis. Like plants, rates and orientations of cellular growth in these organisms depend on fibers in the wall or cell cortex that resist turgor. Controlled fiber sliding may play a key role, though in animals such sliding can be driven actively as well as passively. In animal tissues where cell rearrangements are limited, as during organogenesis, growth coordination and tissue stresses may operate similarly to plants. Thus, although the molecular players controlling plant, animal and microbial development are different, the mechanics of morphogenesis may share common principles.

Figure and caption

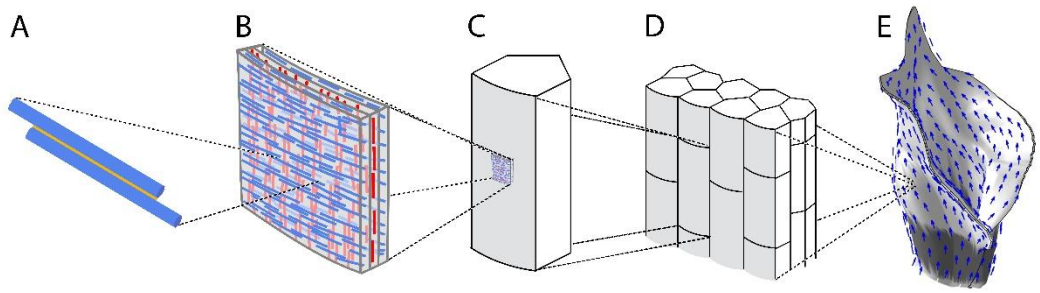

Plant morphogenesis, from nano- to macroscale.

Growth begins with sliding of cellulose fibers **(A)** within the cohesive, extensible and layered networks of cell walls **(B**, layers with different fiber orientations color-coded**)**. Sliding is physically driven by turgor pressure, which generates stress patterns in cells **(C)** and across tissues **(D)**. Patterned tissue growth may be oriented by polarity fields (arrows) to generate complex forms **(E)**. Credit, Enrico Coen.